energies

MDPI

Article

A Practical Approach to Optimising Distribution Transformer Tap Settings †

Joshua Paoli [1], Bernd Brinkmann [2] and Michael Negnevitsky [1,*]

1 School of Engineering, University of Tasmania, Hobart 7001, Australia; joshua.paoli@utas.edu.au
2 TasNetworks, Lenah Valley 7008, Australia; bernd.brinkmann@utas.edu.au
* Correspondence: michael.negnevitsky@utas.edu.au

† The present work is an extension of the paper "Optimising low-voltage transformer tap settings in distribution networks" presented to the 29th Australasian Universities Power Engineering Conference (AUPEC), Nadi, Fiji, 26–29 November 2019, and published in IEEE.

Received: 24 August 2020; Accepted: 15 September 2020; Published: 18 September 2020

Abstract: This paper proposes a method of determining the optimal tap settings for no-load distribution transformers with tap-changing capabilities that is practical to apply in real distribution networks. The risk of low voltage distribution networks violating voltage constraints is impacted by the increasing uptake of distributed energy resources and embedded generation. Some of this risk can be alleviated by suitably setting no-load transformer tap settings, however, modifying these taps requires customer outages and must be infrequent. Hence, loading over the entire year must be considered to account for seasonal variations when setting these taps optimally. These settings are determined using evolution strategy optimisation based on an average loading case. Monte Carlo simulations are used to calculate the probability that the terminal voltages on the distribution transformer secondary terminals violate the network voltage limits when the optimal set of taps for the average case is applied over a whole year. This algorithm was tested on several cases of a real distribution feeder of varying complexity, and produces a sufficiently-optimal set of taps without significant computation time.

Keywords: no-load tap-changing transformers; optimisation; evolution strategy; distribution network utilisation; network planning

1. Introduction

No-load tap-changing (NLTC) transformers comprise the vast majority of transformers in distribution networks with adjustable taps due to their low cost and large number [1,2]. Prior to the widespread increase in distributed energy resources (DERs), NLTC transformer taps have been set to boost the secondary voltage as the unadjusted voltage magnitude decreases with electrical distance from the substation. This is especially prevalent at the end of long distribution feeders. Since the taps must be fixed at installation and usually require a customer outage to be changed, this has historically allowed the voltage at the customer connection point to remain within the regulated voltage bandwidth. Even in instances where the medium voltage (MV) level decreases to near the lower regulatory limit, the customer voltage may remain well within constraints.

The recent uptake of DERs such as solar photovoltaics (PV) and wind generation presents an emerging issue [3]. Distribution networks exhibit high R/X ratios, and as a result of distributed generation injecting power into the low voltage (LV) and MV network, voltages at the connection points to distribution networks can significantly increase [4]. During off-peak periods, the upper voltage limit is at risk of being exceeded [4–6]. Furthermore, unlike in high voltage (HV) networks, determining the scale and severity of this issue in MV and LV networks is a difficult problem. The low number of buses and high number of redundant measurements in HV networks generally result in a well-known HV network state [7]. MV networks, and, to a greater extent, LV networks, have very

few measurements due to the installation and maintenance cost of measurement devices [8], yet these networks are affected disproportionately by this emerging problem. Additionally, high R/X ratios in MV and LV networks reduce the effectiveness of voltage control by reactive power [9]. Therefore, voltage rise must be dealt with pre-emptively, otherwise distribution network operators will be unable to effectively manage voltage rise in distribution networks. Historical loading information obtained through supervisory control and data acquisition (SCADA) systems is readily available to distribution network operators and typically of good quality. Hence, using this data to set NLTC transformer taps to suitable positions based on all possible loading regimes within any given year can assist maintaining the network voltages within admissible limits cost-effectively over longer time periods. Furthermore, with improved distribution network observability and robust distribution state estimation, more data will become available to distribution network operators to improve confidence in the network state and the influence of NLTC transformer tap settings [10–12].

This paper presents the practical method of determining a suitably-optimal set of NLTC transformer taps proposed in [1] applied to additional case studies to demonstrate its applicability to real distribution networks. The optimisation procedure is based on an evolution strategy (ES). ESs are a subset of evolutionary computation that are applied to extremise technical problems where a purely numerical optimisation method is necessary [13]. ESs are simple and perform well with various network models. As a result, an ES is applied to produce an optimal solution for this problem.

Australian Standard AS6100.3.100 specifies the percentage of time that the voltage of phase-to-neutral connections must be within a stipulated voltage percentile [14]. The time for which the LV network exists outside this percentile must be minimised by the proposed optimisation algorithm. The percentage of time that the network voltages are within acceptable limits is then determined by applying Monte Carlo simulations. Proof of concept for this algorithm was presented in [1]. This research applied the algorithm to three case studies of a real Tasmanian distribution feeder that was modified to account for varying network complexity.

2. Materials and Methods

2.1. Evolution Strategy Optimisation

ESs improve a fitness function iteratively through selection and mutation operations. Selection operators randomly select the input parameters at each iteration (referred to as a generation) that undergo mutation of their current value. Mutation operators then sample a normal distribution with zero mean and some appropriate standard deviation and add this to the selected input parameters [15,16]. Following these operations, the output is recalculated, and the new set of input parameters is used in the next generation if the fitness function improves. This method of varying the input parameters slightly and recalculating the fitness function of the output is the basis of the ES algorithm. Several variants of ES have been used to solve a variety of optimisation problems, however, the single parent–single offspring search is the most effective version suggested by experiments [15]. This is termed a (1 + 1)-evolution strategy.

To optimise the transformer tap settings, each MV/LV transformer tap position is input at each iteration and undergoes selection and mutation. The standard deviation (σ_t) of the additive mutation is established initially ($\sigma_t{}^1$), and can be updated as the number of generations increases. This reduces the size of the search space as the solution approaches its optimum (note that σ_t is the same for all input parameters). The 1/5th success rule is most commonly implemented to modify σ_t [13]. Let P be the proportion of generations where the parent parameters are replaced by the offspring parameters to the number of generations in some interval T, then the standard deviation updates according to:

$$\sigma_t^{T+1} = \begin{cases} c.\sigma_t^T, & if\ P < \frac{1}{5} \\ \sigma_t^T, & if\ P = \frac{1}{5} \\ \frac{1}{c}.\sigma_t^T, & if\ P < \frac{1}{5} \end{cases}, \quad (1)$$

where c is an accelerating constant typically in the range $1 < |c| < 1.05$, implemented for improved efficiency.

At each iteration m, the transformer tap positions are randomly adjusted by adding ${\sigma_t}^m$ and rounding the result to the nearest whole tap value in the defined tapping range of each MV/LV transformer. A new load flow is required to recalculate the voltages at each of the secondary terminals of the distribution transformers. Without modification, this approach would likely suffer from impractically long computation time due to the large number of power flow calculations, especially as the size of the network increases. However, adjusting any given transformer tap in a network is not predicted to significantly alter the results of the power flow. Therefore, fewer power flows are required than the total number of generations. Let k be the number of generations at which a new power flow is executed, given by:

$$k = 0.5N_{gen} + a \times 0.05N_{gen}, \tag{2}$$

where N_{gen} is the total number of generations for which the algorithm runs and $a = 0, 1, 2, \ldots, 10$.

Metrics justifying the reduced number of power flows were devised in [1] to demonstrate the variation in the voltages for successive power flows is insignificant as assumed, particularly as the tap positions approach the optimal solution. If this assumption holds, the solution is optimised in only a small number of power flows, reducing the overall computation time dramatically. The average error and maximum error between power flows are calculated to demonstrate this assumption. Let $\overline{\Delta}$ be the average error between load flows, defined as:

$$\overline{\Delta} = \frac{\sum_{i=1}^{n}\left|V_i^{k+1} - V_i^{k}\right|}{n}. \tag{3}$$

Let Δ_{max} be the maximum error between load flows, defined as:

$$\Delta_{max} = max\left(\left|V_i^{k+1} - V_i^{k}\right|\right). \tag{4}$$

Here, n is the number of MV/LV transformers in the network and ${V_i}^k$ represents the voltage at bus i following tap setting optimisation in power flow k.

Since the solution commences with a randomised set of taps, the average error between consecutive power flows is initially expected to be large. However, as subsequent power flows run at iteration k are not predicted to significantly vary the solution, the average error should decrease with the number of power flows. Once $\overline{\Delta}$ reaches a small, steady-state value, each successive power flow only slightly varies the network state since the set of transformer taps is approaching the optimal set.

The maximum error Δ_{max} should also decrease initially. If subsequent power flows cause previously compliant voltages to approach or exceed voltage limits as the solution is updated, or cause variations in extreme voltages, the maximum error will change significantly. If the algorithm is converging on the optimal set, the maximum error will remain reasonably constant.

2.2. Objective Function

The objective function F to be minimised is defined as:

$$F = \frac{\sum_{i=1}^{n}\left|V_i - V_{set,i}\right|^2}{n}, \tag{5}$$

where V_i represents the voltage at the secondary terminal of MV/LV transformer i, and n refers to the total number of MV/LV transformers that are undergoing optimisation. F is the sum of squared differences between the voltages calculated at the LV terminals and some setpoint $V_{set,i}$ within the required voltage range that can be fixed for each transformer. For this research, $V_{set,i}$ is set to 1 p.u., the nominal system voltage, although this can be adjusted as necessary. Note that the fitness function is given by $1/F$ and must be maximised.

The objective function is quadratic, since most voltages along the feeder are likely near $V_{set,i}$ and therefore within constraints. Any voltages that are far from $V_{set,i}$ and therefore close to or exceeding the voltage limits will disproportionately increase the objective function. This contrasts with a linear objective function that risks masking the impact of non-compliant voltages on F since their number is expected to be small compared to the total number of optimised voltages in the network [1].

2.3. Load Partitioning and Monte Carlo Simulations

As shown in Figure 1, the method proposed in [1] divides the infeeder loading into three partitions. This is determined from the historical measurement of the infeeder current magnitude over one year. If I_{max} is the maximum infeeder current magnitude for the year, then partition C_1 represents all loading cases where the infeeder current I is in the range $0 < I \leq 1/3 \times I_{max}$, C_2 represents all cases for $1/3 \times I_{max} < I \leq 2/3 \times I_{max}$, and C_3 represents all cases for $2/3 \times I_{max} < I \leq I_{max}$.

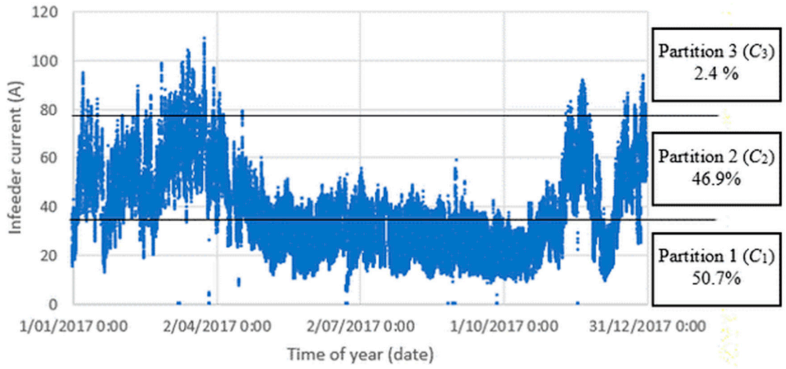

Figure 1. Historical infeeder loading data for the real distribution network analysed in the case studies. Load partitions are shown, as well as the percentage of time for which they occur.

The partition containing the highest measurement count represents the current magnitude range that flows through the substation for the largest percentage of the year. The average within this partition is the infeeder current that is divided amongst each of the load buses in the network using a load allocation method (in this case, PSS SINCAL). The optimal tap positions are calculated for this loading case. Furthermore, to account for the random nature of the ES, the optimal tap positions are calculated three times for randomly determined initial tap settings. The objective function of the median tap positions across these trials is then calculated and compared to the objective function of each individual trial. The set of taps that produce the minimum objective function corresponds to the optimal set of taps for the network under this loading case. This method is preferred to selecting the average infeeder current to allocate loads as it is more robust against extreme loading cases.

Once calculated, these tap settings are applied to each of the original loading partitions to examine how the settings perform over an entire year. Since loads vary, Monte Carlo simulations can be used to capture this performance. The historical infeeder loading data can be sampled and allocated to the network buses. Each loading partition is sampled separately. The risk of voltage violation is then calculated, and is defined as the percentage of time the feeder would have voltages outside voltage constraints when the optimal tap settings are applied.

Consider partitions C_1, C_2 and C_3 which make up x%, y% and z% of the historical infeeder loading throughout one year respectively. The average infeeder loading of the partition with the highest percentage is calculated. This average is used to allocate the load on each bus using a load allocation scheme, and the subsequent network loading is used to calculate the optimal tap settings. Then, N_{max} Monte Carlo simulations are completed by applying the optimal set of taps to sample loading scenarios from each partition separately. For each simulation, let N_1, N_2 and N_3 be the number of simulations that fall outside the voltage constraints for partitions C_1, C_2 and C_3, respectively. Then, the risk R of the feeder violating constraints with the optimal set of taps as a percentage is:

$$R = x \times \frac{N_1}{N_{max}} + y \times \frac{N_2}{N_{max}} + z \times \frac{N_3}{N_{max}}. \quad (6)$$

2.4. Algorithm Description

The algorithm was originally described in [1]. A flow chart of this algorithm is given in Figure 2, and consists of the following general steps:

1. Parameters required for optimisation are defined, and the network is initialised with the network loading as described in Section 2.3. The transformer tap settings are all randomised.
2. A (1 + 1)-Evolution Strategy is implemented to produce a set of transformer taps that sufficiently optimise the objective function F. Load flows are not computed at each generation, but are instead calculated at strategic intervals according to Equation (2) to improve the computation time. Three sets of transformer taps are calculated by completing this step three times.
3. A fourth set of transformer taps is established by calculating the median tap setting for each transformer from each of the three trials. Its objective function is compared to the objective functions computed from the result of each of the trials. The lowest objective function corresponds to the set of taps that best optimise the network for the average loading case.
4. The tap settings are applied to the network. Monte Carlo simulations are then applied as described in Section 2.3 to determine the likelihood of voltage violations throughout the time period given by the data for each of the loading partitions. The risk of voltage violations R is then calculated from the results of the Monte Carlo simulations using Equation (6).

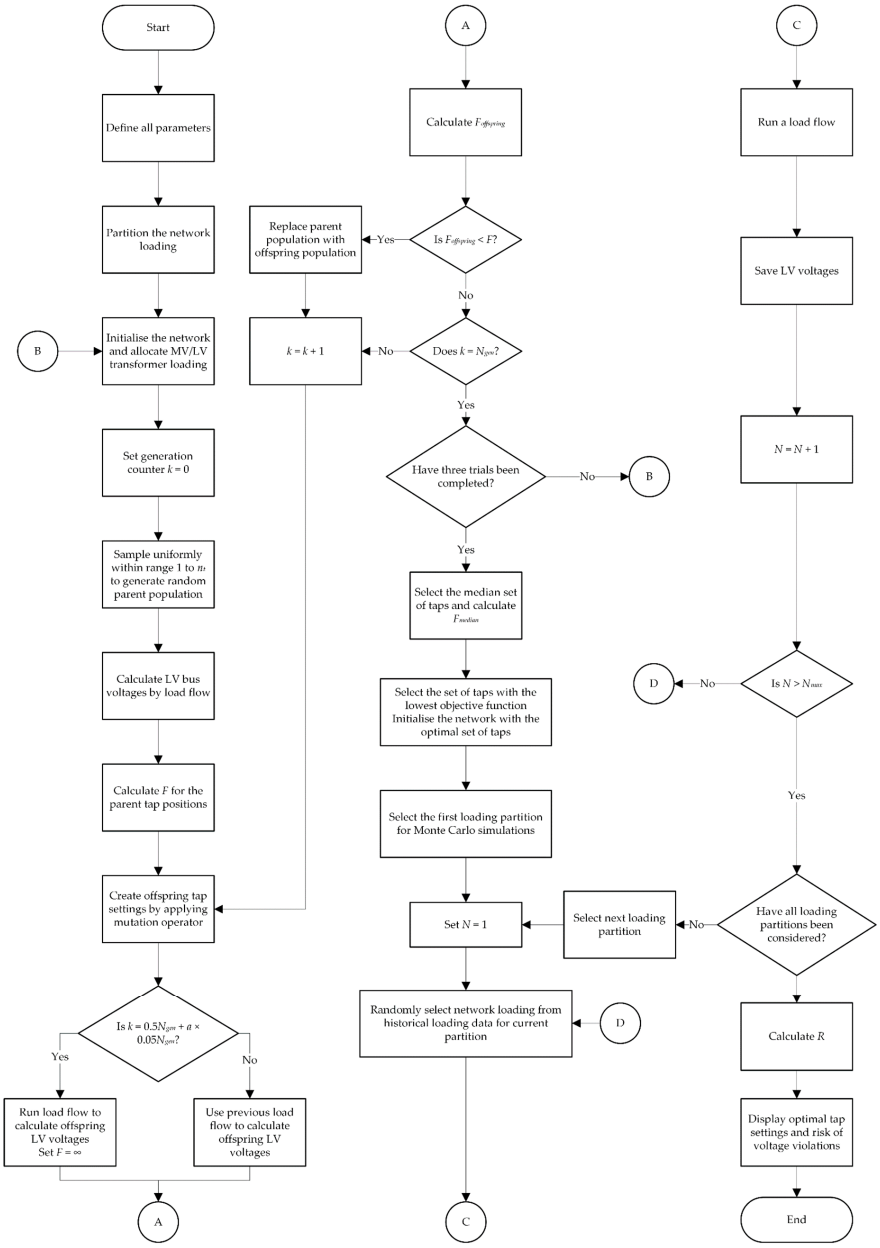

Figure 2. Flow chart of the algorithm. Reproduced from [1], IEEE: 2019.

3. Results

3.1. Seven-Bus Test Network

Proof of concept of the algorithm was achieved using the seven-bus test network shown in Figure 3, and results were presented in the original conference paper [1]. All distribution lines are assumed to have the same conductor type and be equally spaced for simplicity. The transformers were modelled with five tap positions, each providing a variation of 2.5% of the nominal voltage. Tap 3 was defined as the neutral tap, providing 0% variation. Note that these tap settings were applied to all case studies. Results for the seven-bus test system confirm that the tap settings produced by the algorithm converge on the optimal tap settings.

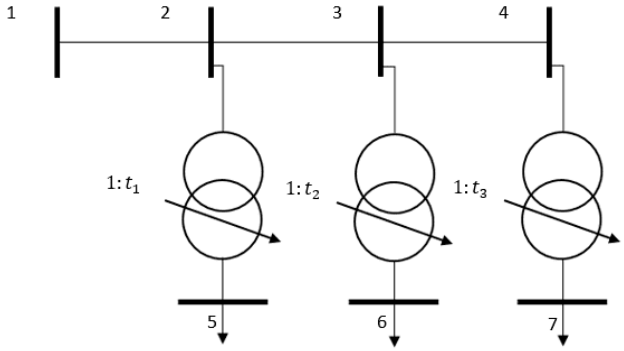

Figure 3. Seven-bus test network for proof of concept.

3.2. Real Distribution Network

The algorithm was tested on variants of a real distribution feeder provided by the Distribution Network Service Provider (DNSP) of Tasmania, Australia, TasNetworks, shown in Figure 4 (Supplementary Materials). The feeder contains a voltage regulator and single-wire earth return (SWER) line (highlighted). The algorithm was run against three test cases of the real distribution network of varying network complexity:

- Case 1: Highly-loaded feeder with the voltage regulator and SWER section bypassed.
- Case 2: Load-partitioned infeed with the voltage regulator and SWER section bypassed.
- Case 3: Load-partitioned infeed with voltage regulator and SWER section unbypassed.

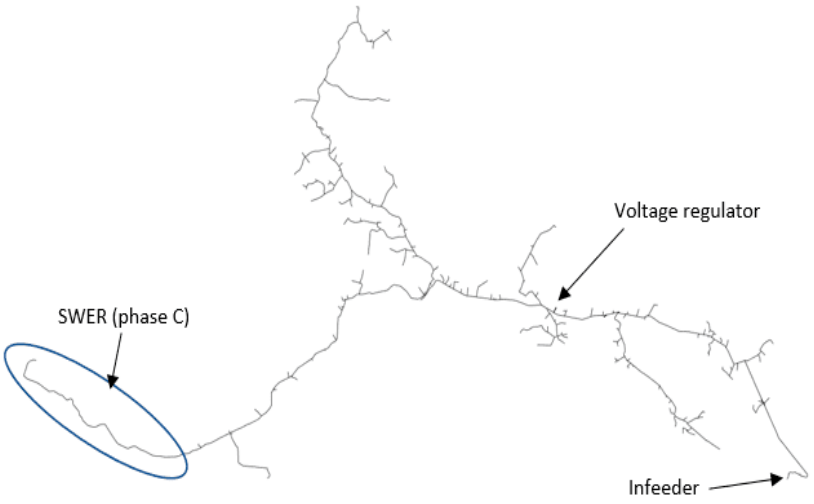

Figure 4. Real distribution feeder network model supplied at 22 kV. The infeeder, voltage regulator and SWER line are shown.

3.2.1. Case 1—Highly-Loaded Feeder with Voltage Regulator and SWER Section Bypassed

Case 1 compared running power flows computed every generation after generation 5000 (denoted Case 1.1) against the algorithm proposed in Section 2.4 (denoted Case 1.2). In particular, computation time and the value of the objective function were compared to demonstrate the practicality of the proposed algorithm.

For simplicity, the infeeder loading was set to 100 A and the infeeder voltage was set to 1.05 p.u. The feeder loading was distributed to the MV/LV transformers proportionally by the transformer kVA rating using the load allocation procedure in PSS SINCAL. This allocation procedure was used for all case studies on the distribution network.

The parameters of the evolution strategy for Case 1.1 are given in Table 1, and for Case 1.2 in Table 2. Case 1.1 ran an initial power flow with randomised tap settings. The voltages were updated according to the algorithm without completing any additional load flows. At 5000 generations, a power flow was computed at every generation to progress toward the optimal solution using a standard evolution strategy approach.

Table 1. Evolution strategy parameters for Case 1.1.

Parameter	Symbol	Value
Number of taps per transformer	n_t	5
Voltage change per tap	t	2.5%
Total number of generations	N_t	10,000
Initial standard deviation	${\sigma_t}^1$	0.3
Target voltage	V_{set}	1 p.u.
Accelerating factor	c	1.02
Acceleration interval	T	50
Lower standard deviation limit	${\sigma_t}^\infty$	0.17

Table 2. Evolution strategy parameters for Case 1.2.

Parameter	Symbol	Value
Number of taps per transformer	n_t	5
Voltage change per tap	t	2.5%
Total number of generations	N_t	30,000
Initial standard deviation	${\sigma_t}^1$	0.3
Target voltage	V_{set}	1 p.u.
Accelerating factor	c	1.02
Acceleration interval	T	30
Lower standard deviation limit	${\sigma_t}^\infty$	0.17

Case 1.2 was executed using the algorithm shown in Figure 2 prior to implementing Monte Carlo simulations, as the feeder network and feeder loading were simplified. A larger number of generations was required for Case 1.2 to ensure each new power flow solution converged with sufficient iterations each time the new load flow solution was calculated. The total number of load flows calculated in each case is the same and, therefore, the computational burden increases only marginally by increasing the total number of generations.

The standard deviation reduces as the solution optimises according to Equation (1). Since there are a finite number of transformers, there is a lower limit of ${\sigma_t}^\infty = 0.17$ that corresponds to an expected value of one for the number of taps that a mutation modifies each generation. With this limit imposed, at least one tap position per generation is expected to be mutated, reducing the chance of redundant iterations.

The objective function at each generation for Case 1.1 is given in Figure 5. Each generation, the set of taps with the lowest objective function is retained and is used to produce the child population. The transformer taps proceed toward the optimal set. However, until the power flows recommence after 5000 generations, the results do not account for the effect of each transformer on every other

transformer in the network. Since changing tap settings does not significantly change the power flows, the tap settings at 5000 generations are closer to the optimal set than the initial set of randomised taps. The minimum objective function for Case 1.1 was 3.4996×10^{-5}.

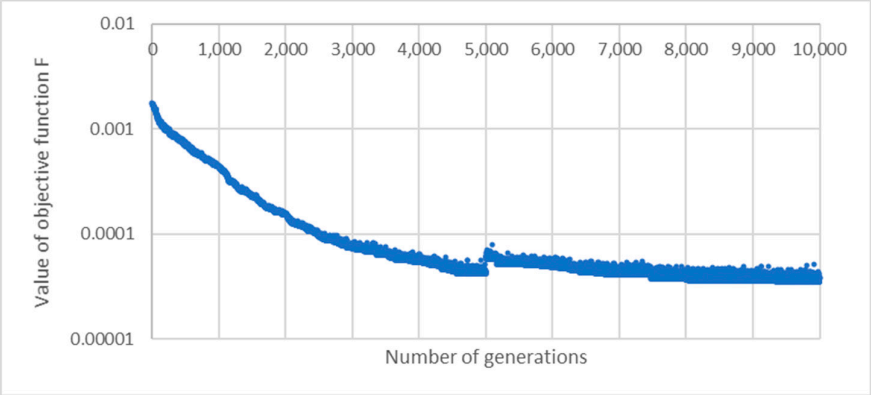

Figure 5. Objective function value against the number of evolution strategy generations for Case 1.1.

The feeder topology is radial, so the medium voltage level begins at 1.05 p.u. at the infeeder and decreases for increasing electrical distance from the infeeder since the voltage regulator has been bypassed. Consequently, the unadjusted secondary voltages are expected to decrease from above V_{set} at the infeeder to below V_{set} at the furthest radial bus. As a result, the taps closest to the infeeder are expected to have the lowest setting to bring the secondary voltage down toward V_{set}, and the taps furthest from the infeeder are expected to require the highest setting. This feature can be seen in Figure 6. Furthermore, the expected secondary voltages still show a decreasing trend with discontinuous jumps. This occurs where a tap position changes compared to the closest upstream transformer (Figure 7).

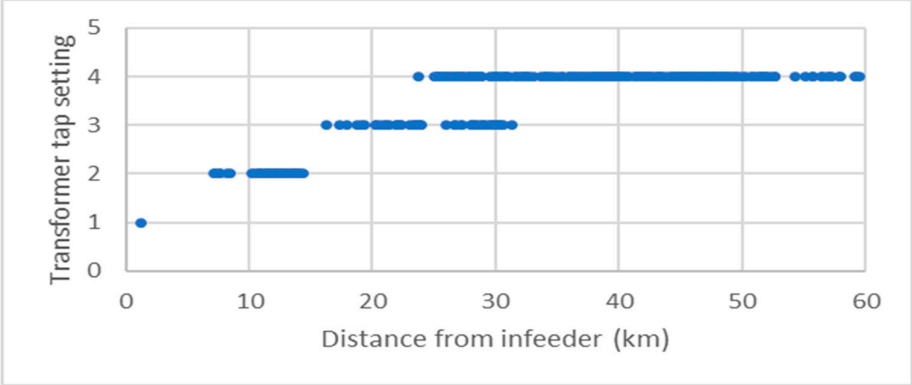

Figure 6. Tap setting against distance from the infeeder for Case 1.1.

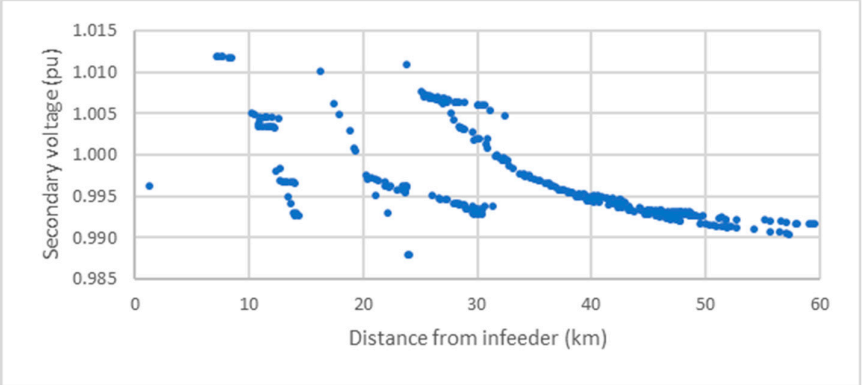

Figure 7. Voltage at the MV/LV transformer terminal against distance from the infeeder for Case 1.1.

These results demonstrate that the unmodified version of the evolution strategy can generate a suitably optimal set of taps for the infeeder loading of 100 A at 22 kV. However, the computation time for this case was recorded as approximately six hours. This is impractical to run on every feeder in a distribution network.

Case 1.2 ran the proposed version of the evolution strategy, with power flows only executed every 1500 generations (Figure 8). The objective function at each generation shows several discontinuous jumps when each new power flow is run.

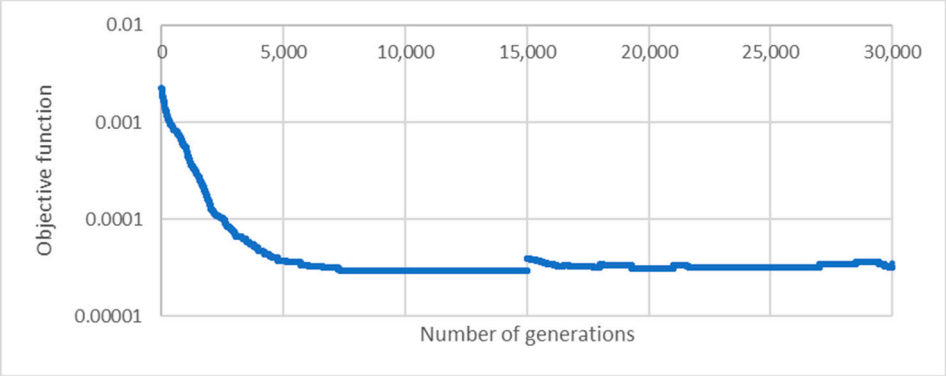

Figure 8. Objective function value against the number of evolution strategy generations for Case 1.2.

Three candidate optimal tap settings were calculated by running three trials from random initial tap settings. The median set of taps was then determined. A final power flow was run on the MV network model to determine the objective function of the median set. This was compared to the objective function of the three individual trials. The objective function for the median tap settings evaluated to 3.4996×10^{-5}, less than all three individual trials and matching the optimal solution produced in Case 1.1 (see Table 3). The computation time for Case 1.2 was approximately one minute, which demonstrates that the proposed algorithm can produce optimal tap settings for simple distribution feeders in a practical amount of time.

Table 3. Final objective function for each trial and the objective function of the median tap settings in Case 1.2.

Trial	Objective Function, F
1	4.8175×10^{-5}
2	4.5943×10^{-5}
3	4.7616×10^{-5}
Median tap settings	3.4996×10^{-5}

Figure 9 shows the average error (Equation (3)) and maximum error (Equation (4)) between successive power flows for each trial in Case 1.2. As the solution proceeds from random toward optimal, the average error initially reduces. Once the tap positions are close to optimal, the average error remains constant. The maximum absolute error remains constant, suggesting that the tap settings are converging on the optimal solution despite power flows only being computed infrequently in accordance with Equation (2).

Furthermore, Figure 10 demonstrates that each trial resulted in a more variable set of taps when compared with the median set. This emphasises the requirement to select the median tap position of multiple ES trials to form the optimal set, as each trial is susceptible to stagnating prematurely in local minima as a result of the random nature of evolution-based optimisation.

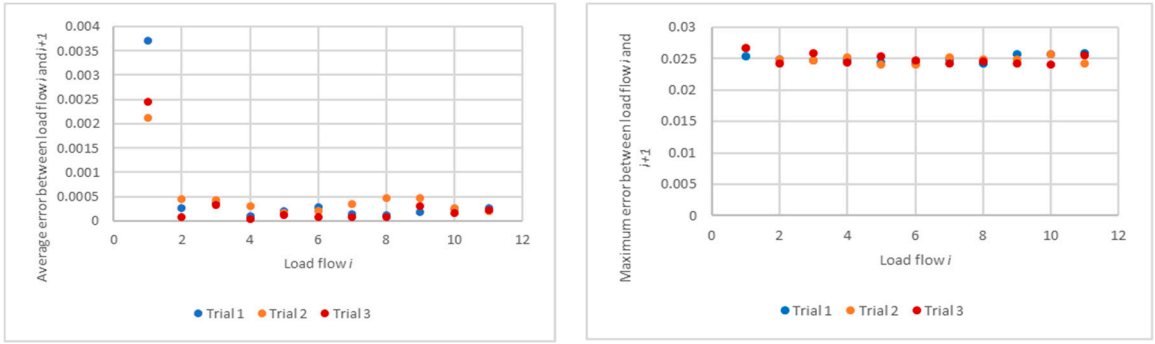

(**a**) (**b**)

Figure 9. Metrics measured for Case 1.2. (**a**) Average error $\overline{\Delta}$ of the secondary voltages between the results of consecutive power flows. (**b**) Maximum absolute error Δ_{max} of the secondary voltages between the results of consecutive power flows.

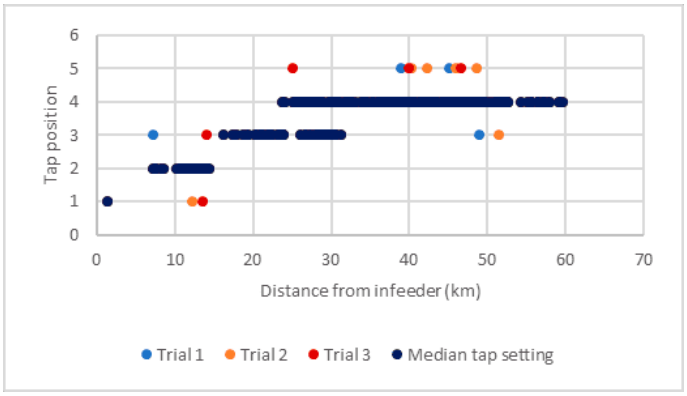

Figure 10. Transformer tap setting against electrical distance from the infeeder for Case 1.2. The median set of taps produced the lowest objective function and is therefore deemed the optimal set.

3.2.2. Case 2—Load-Partitioned Infeed with the Voltage Regulator and SWER Section Bypassed

Case 2 used historical SCADA measurement data for the current and voltage magnitudes at the infeeder to determine the optimal set of transformer taps. Figure 1 shows the measured infeeder current for a whole year, as well as the partitions as described in Section 2.3. The longest-occurring partition was C_1. The average of this partition produced an infeeder loading of 18.4 A at 22 kV. The load allocation method in PSS SINCAL was then applied to apportion this loading to each MV/LV transformer in the network model based on their kVA rating. The optimal tap settings were calculated for this case. An infeeder voltage of 1.02 p.u. was applied. This was calculated by averaging the historical data for the infeeder voltage.

This case also compared calculating power flows at each generation after generation 5000, denoted Case 2.1, against the Algorithm in Section 2.4, denoted Case 2.2. Case 2.1 used the ES parameters in Table 1 and Case 2.2 used the ES parameters in Table 2. Again, Case 2.1 required approximately six hours to run to completion, and Case 2.2 required approximately 1 min.

Figure 11 demonstrates the optimal set of transformer taps calculated for Case 2.1. The final value of the objective function was 8.2170×10^{-5}. The corresponding secondary voltage profile is shown in Figure 12.

Case 2.2 ran the algorithm described in Section 2.4. As shown in Figure 2, the algorithm generates three sets of tap positions, and the median tap settings of all three runs is taken as the proposed optimal. The optimal tap settings for Case 2.2 are shown in Figure 13, and the secondary voltage profile for Case 2.2 is shown in Figure 14. Again, the three individual trials in Case 2.2 did not independently produce solutions better than Case 2.1, however the median of these three runs resulted in a fitness

better than in Case 2.1. The objective function for Case 2.2 was 8.1688×10^{-5}. For simple distribution networks, this algorithm has produced sufficiently optimal results with practical computation time.

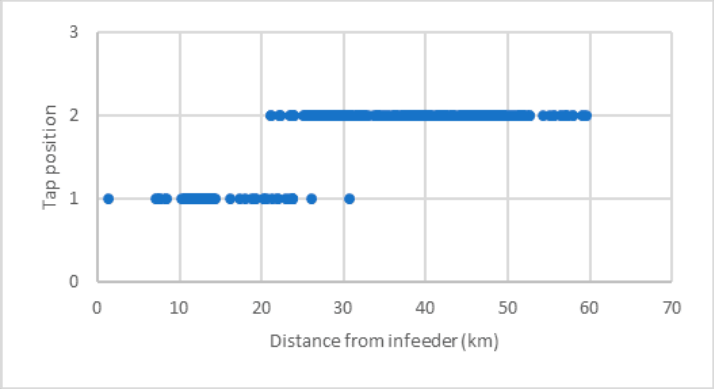

Figure 11. Transformer tap setting against electrical distance from the infeeder for Case 2.1.

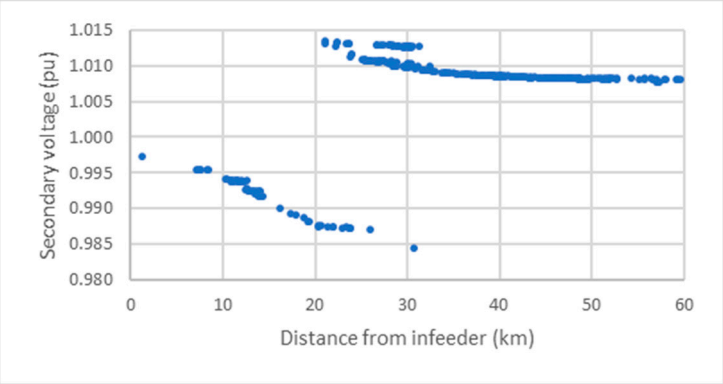

Figure 12. Secondary terminal voltage profile for MV/LV transformers for Case 2.1.

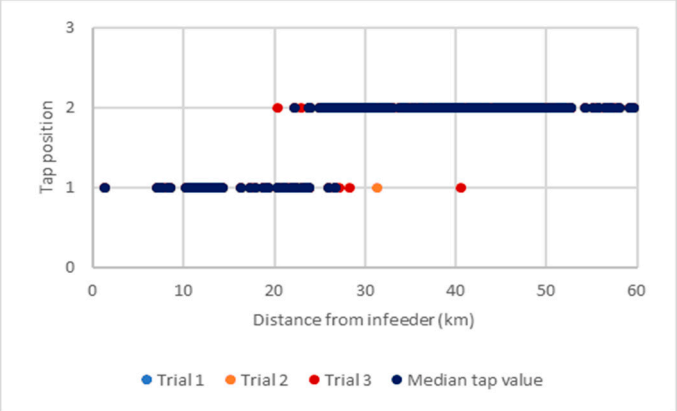

Figure 13. Transformer tap setting against transformer distance from the infeeder for Case 2.2.

The average error and maximum error for Case 2.2 are provided in Figure 15. The average error demonstrates that successive power flows are proceeding toward the optimal set of taps. The maximum error provides evidence to suggest why Case 2.1 was unable to find a set of taps with a fitness function less than or equal to Case 2.2. The optimal solution is close to several local minima in the problem space. Since Case 2.2 completes an ES multiple times, the median tap positions are more robust against becoming trapped in local minima. Ideally, Case 2.1 would be repeated to account for the random input tap settings, however, the excessive run time makes this approach impractical.

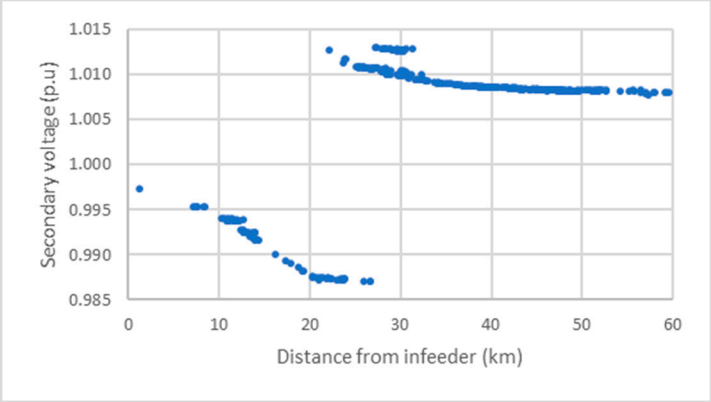

Figure 14. Secondary terminal voltage profile for MV/LV transformers for Case 2.2. The result had a better fitness than Case 2.1.

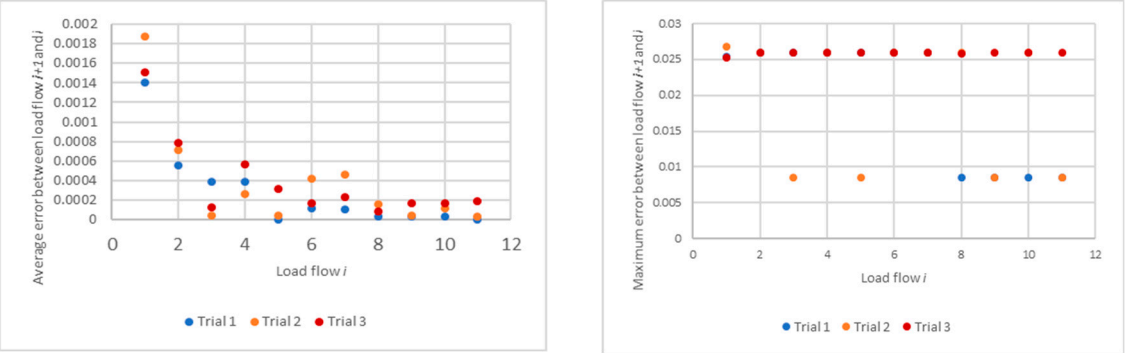

(**a**) (**b**)

Figure 15. Metrics measured for Case 2.2. (**a**) Average error $\overline{\Delta}$ of the secondary voltages between the results of consecutive power flows. (**b**) Maximum absolute error Δ_{max} of the secondary voltages between the results of consecutive power flows.

3.2.3. Case 3—Load-Partitioned Infeed with the Voltage Regulator and SWER Section Included

The distribution network in Figure 4 also contains a voltage regulator and SWER-connected transformer. These features are often neglected in literature to simplify the analysis of distribution networks. The approach proposed in Section 2.4 does not require analytical optimisation, and therefore the SWER line and voltage regulator can be included in the network model during ES optimisation, which was completed in this case study.

The load for this case was allocated as in Case 2, with the historical infeeder current being partitioned to produce an average case to optimise. The load allocation method in PSS SINCAL was then applied to apportion the infeeder loading of 18.4 A at 22 kV to the MV/LV transformer LV terminals.

Phase C is connected to the SWER section in the network model and was therefore analysed in this case. The voltage profile calculated at the LV transformer terminals is shown in Figure 16, and the optimal taps for each transformer are shown in Figure 17. The voltage regulator is downstream of a 6 km spur (see Figure 4). The MV voltages of transformers downstream of the regulator have been boosted. The MV voltages of transformers on the 6 km spur have not. Therefore, the primary voltage is lower for these transformers than others at equal electrical distance from the infeeder. As a result, tap position 3 is maintained by transformers on this spur to produce secondary voltages closer to 1 p.u., despite other transformers being set at tap position 2 at an equal distance. The results for transformers on the spur are explicitly highlighted in Figures 16 and 17.

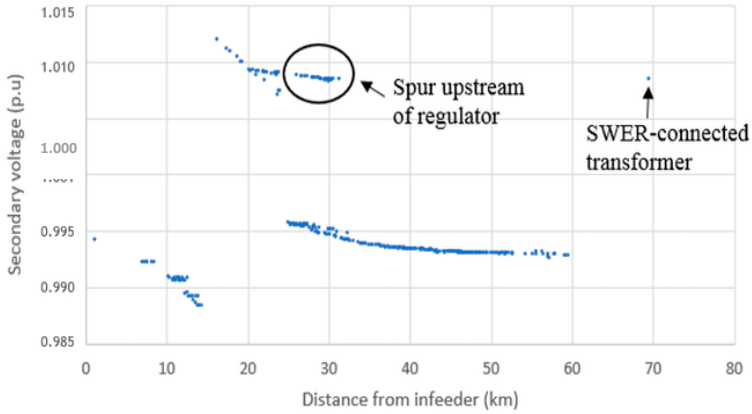

Figure 16. Secondary terminal voltage against electrical distance from the infeeder for MV/LV transformers for Case 3.

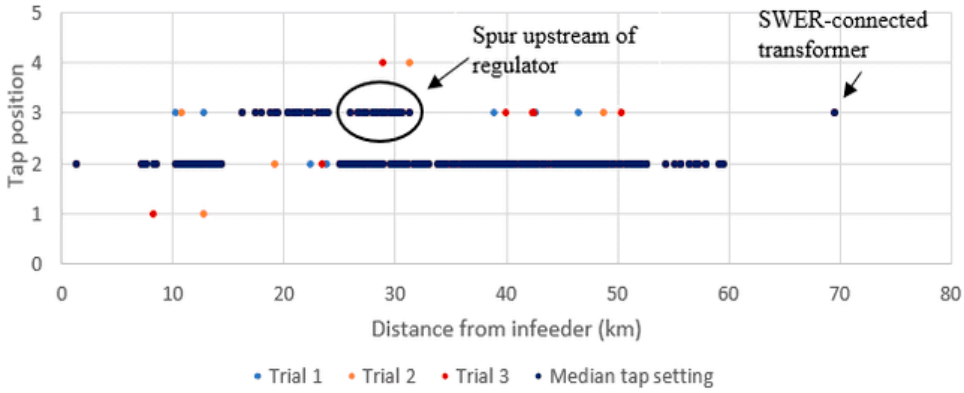

Figure 17. Transformer tap setting against electrical distance from the infeeder for Case 3. The median set of taps produced the lowest objective function and is, therefore, deemed the optimal set.

As for the previous cases, three candidate sets of optimal taps were determined by running three trials. The median tap position of the three trials for each transformer was determined and the corresponding objective function calculated. This objective function evaluated to 5.574×10^{-5}, less than the objective functions of the three individual trials. Figure 17 shows that the median set of taps has removed the variability produced by the three individual trials, again demonstrating the requirement for the optimal set to be selected by considering the median tap settings as well as the settings for each trial individually.

The average and maximum absolute error between successive power flows for each trial is given in Figure 18. As the solution proceeds from random toward optimal, the average error initially reduces. Once the tap positions are near-optimal, the average error remains constant. The maximum absolute error also decreases between the first and second load flows before remaining constant, suggesting that the solution is converging on the optimal tap settings despite infrequent power flow computations. In this instance, owing to the voltage regulator, the computation time was approximately 2.5 min.

The risk of the feeder violating voltage constraints over an entire year with the optimal tap settings applied was calculated. One thousand Monte Carlo simulations were run for each loading partition. This determined the percentage of time for which the LV voltage levels violated constraints. Table 4 shows the percentages for these partitions. The feeder experiences the minimum loading for the maximum time (see Figure 1). The corresponding partition was used to determine the loading applied to the network that the ES optimised. This load partition produced no violations for all 1000 Monte Carlo simulations, as did the second partition. The maximum loading partition, which covered 2.4% of the historical data, exceeded constraints 22.5% of the time. Hence, the overall risk of voltage violation for this network was 0.54%, found by applying Equation (6). This corresponds to the feeder being within

limits for 99.46% of the year. Figure 19 shows where voltage violations on the feeder would likely occur when subjected to maximum loading with the optimal tap settings applied. Immediately upstream of the voltage regulator, the network exceeded the lower voltage limit. Immediately downstream of the voltage regulator, the upper voltage limit was exceeded.

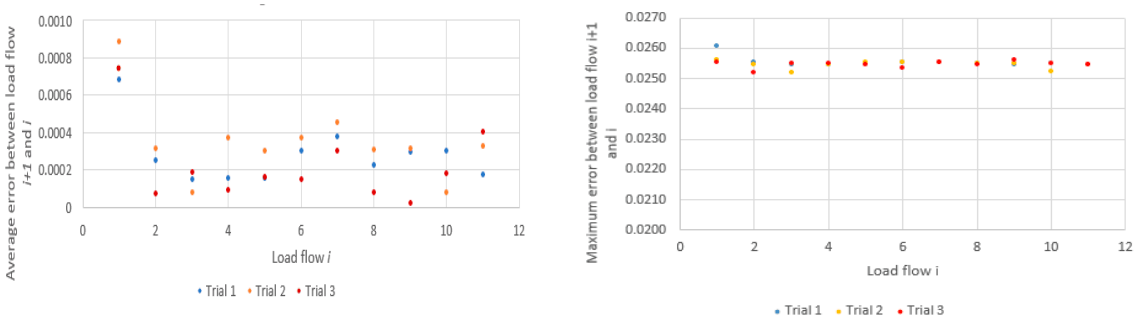

(**a**) (**b**)

Figure 18. Metrics calculated for Case 3. (**a**) Average error $\overline{\Delta}$ of the secondary voltages between the results of consecutive power flows. (**b**) Maximum absolute error Δ_{max} of the secondary voltages between the results of consecutive power flows.

Table 4. Results of Monte Carlo simulations for each partition in Case 3.

Partition Number	Percentage of Time Partition Exists on Network	Percentage of Time Partition Is Outside Regulated Constraint
1	50.7%	0%
2	46.9%	0%
3	2.4%	22.5%

Figure 19. Real distribution feeder with regions of compliance (green), undervoltage (red) and overvoltage (blue) highlighted for the maximum loading case on the network with the optimal tap settings applied.

4. Conclusions

This paper has identified a (1 + 1)-evolution strategy as a powerful and viable method for producing optimal tap positions for NLTC distribution transformers under an average loading condition. Power flow calculations were only completed after a certain number of generations had elapsed, which allowed the algorithm to execute in a practical amount of time. This succeeded because variations in tap positions did not significantly change the MV network power flows. This was confirmed by the average error and maximum absolute error defined in Equations (3) and (4)

respectively. Since the objective function could become trapped in local minima, multiple trials were implemented in each case that the ES was optimising. The median tap position of each transformer in these trials was chosen to produce a candidate set of optimal tap positions. This was confirmed by comparing the objective function of each trial with that of the corresponding median set of taps. In each case, the median set of taps corresponded to the most optimal set of taps found by the algorithm, and a sufficiently-optimal set of taps for the network overall.

The results have shown that the proposed procedure is applicable where substation information and a network model are available, regardless of the complexity of the model. Case 1 demonstrated the significant improvement in computation time associated with the algorithm. This result establishes an ES as a practical procedure for optimising radial distribution transformer tap settings. Case 2 provides evidence that this procedure can then be applied to determine appropriate tap settings for real distribution networks using historical loading data obtained through existing SCADA systems, further establishing the practicality of the method.

This approach was shown to produce an acceptable solution with SWER line and voltage regulators in the MV network model. These components add complexity to the network analysis, and are often neglected in the literature. Case 3 identified an adverse effect on the convergence and computation time of each trial of the ES due to the voltage regulator. However, the developed methodology could still determine a suitably optimal set of taps by taking the median set of taps from all trials. The impact of the SWER line on the effectiveness of the algorithm in this single-phase study was found to be negligible. However, this particular configuration must be considered carefully if any future research intends to apply this method to three-phase studies [17]. Furthermore, a clustering method such as K-means may be applied to cluster the active power, reactive power and historical voltage of the feeder. A weighted average of the corresponding clusters can then be calculated to determine a representative loading that may better select tap positions that account for the severity of voltage violations in extreme cases. This is subject to further research.

The load partitioning method used was simple and efficient. Monte Carlo simulations were introduced to determine whether partitioning the load in this manner was successful. The simulations confirmed that the network was maintained within the required voltage constraints for 99.5% of the year with the optimal tap settings generated in Case 3. Hence, the method overall has successfully determined a set of NLTC transformer taps that would minimise the risk of the network violating the voltage requirement stipulated by AS6100.3.100. This has been achieved without significant computation time. Whether a given distribution feeder always meets the 99th percentile constraint stipulated in the Australian Standard depends on the topology, components and loading of the network being studied. In cases where violation is likely, or even inevitable, this approach may provide a network planning tool to identify possible sections of networks that require augmentation.

Supplementary Materials: The following are available online at http://www.mdpi.com/1996-1073/13/18/4889/s1, Substation data availability is subject to approval from TasNetworks. PSS SINCAL is licensed power system analysis software. The remaining code was written in Excel Visual Basic 16.0.

Author Contributions: Conceptualization: M.N. and J.P.; methodology: J.P. and B.B.; software: J.P.; validation: J.P., B.B. and M.N.; formal analysis: J.P.; investigation: J.P. and B.B.; resources: J.P. and B.B.; data curation: J.P.; writing—original draft preparation: J.P.; writing—review and editing: J.P., B.B. and M.N.; visualization: J.P. and B.B.; supervision: M.N. All authors have read and agreed to the published version of the manuscript.

Funding: This research received no external funding.

Acknowledgments: We kindly acknowledge the assistance, expertise and support provided by the Network Performance team at TasNetworks, with special thanks to James Lord, George Ivokvic and Chris Wembridge.

Conflicts of Interest: The authors declare no conflict of interest.

References

1. Paoli, J.; Brinkmann, B.; Negnevitsky, M. Optimising low-voltage transformer tap settings in distribution networks. In Proceedings of the 29th Australasian Universities Power Engineering Conference (AUPEC), Nadi, Fiji, 26–29 November 2019. [CrossRef]
2. Aziz, T.; Ketjoy, N. Enhancing PV penetration in LV networks using reactive power control and on load tap changer with existing transformers. *IEEE Access* **2018**, *6*, 2683–2691. [CrossRef]
3. Haque, M.M.; Wolfs, P. A review of high PV penetrations in LV distribution networks: Present status, impacts and mitigation measures. *Renew. Sustain. Energy Rev.* **2016**, *62*, 1195–1208. [CrossRef]
4. Masters, C.L. Voltage rise: The big issue when connecting embedded generation to long 11 kV overhead lines. *Power Eng. J.* **2002**, *16*, 5–12. [CrossRef]
5. Priye, A.; Komla, K. Voltage rise issue with high penetration of grid connected PV. *IFAC Proc. Vol.* **2014**, *47*, 4959–4966. [CrossRef]
6. Alam, M.J.E.; Muttaqi, K.M.; Sutanto, D. A comprehensive assessment tool for solar PV impacts on low voltage three phase distribution networks. In Proceedings of the 2nd International Conference on the Developments in Renewable Energy Technology (ICDRET 2012), Dhaka, Bangladesh, 5–7 January 2012; pp. 1–5.
7. Abur, A.; Exposito, A.G.A. *Power System State Estimation Theory and Implementation*, 2nd ed.; Marcel Dekker, Inc.: New York, NY, USA, 2004.
8. Feng, H.; Babizki, A.; Breker, S.; Rudolph, J. Intelligent control of on-load tap-changer based on voltage stability margin estimation using local measurements. In Proceedings of the Cigre SC-C6, Paris, France, 21–26 August 2016; pp. 952–955.
9. Kryonidis, G.C.; Demoulias, C.S.; Papagiannis, G.K. A probabilistic evaluation of voltage control strategies in active MV networks. In Proceedings of the 52nd International Universities Power Engineering Conference (UPEC), Heraklion, Greece, 28–31 August 2017; pp. 1–6. [CrossRef]
10. Brinkmann, B.; Negnevitsky, M. A probabilistic approach to observability of distribution networks. *IEEE Trans. Power Syst.* **2017**, *32*, 1169–1178. [CrossRef]
11. Brinkmann, B.; Negnevisky, M. A practical approach to observability analysis and state estimation in distribution networks. In Proceedings of the 2016 IEEE Power and Energy Society General Meeting (PESGM), Boston, MA, USA, 17–21 July 2016; pp. 1–5. [CrossRef]
12. Brinkmann, B.; Negnevisky, M. Robust state estimation in distribution networks. In Proceedings of the 2016 Australasian Universities Power Engineering Conference (AUPEC), Brisbane, Australia, 25–28 September 2016; pp. 1–5. [CrossRef]
13. Back, T.; Hoffmeister, F.; Schwefel, H.P. A survey of evolution strategies. In Proceedings of the fourth international conference on genetic algorithms, San Diego, CA, USA, 13–16 July 1991.
14. Standards Australia. *Electromagnetic Compatibility (EMC) Part 3. 100: Limits—Steady State Voltage Limits in Public Electricity Systems*; Standards Australia: Sydney, Australia, 2011.
15. Negnevitsky, M. *Artificial Intelligence: A Guide to Intelligent Systems*, 2nd ed.; Pearson Eduction Limited: Harlow, UK, 2005.
16. Beyer, H.; Schwefel, H.P. Evolution strategies—A comprehensive introduction. *Nat. Comput.* **2002**, *1*, 3–52. [CrossRef]
17. Brinkmann, B.; Bicevskis, K.; Scott, R.; Negnevitsky, M. Evaluation of single- and three-phase state estimation in distribution networks. In Proceedings of the 2017 Australasian Universities Power Engineering Conference (AUPEC), Melbourne, Australia, 19–22 November 2017; pp. 1–5. [CrossRef]